Advanced Composite Materials
Publication details, including instructions for authors and subscription information:
http://www.tandfonline.com/loi/tacm20

A Probabilistic SCG Model for Transverse Cracking in CFRP Cross-ply Laminates under Cyclic Loading

Keiji Ogi [a] , Shinji Ogihara [b] & Yashiro Shigeki [c]
[a] School of Science and Engineering, Ehime University, 3, Bunkyo-cho, Matsuyama, Ehime 790-8577, Japan;, Email: kogi@eng.ehime-u.ac.jp
[b] Faculty of Science and Technology, Tokyo University of Science, 2641, Yamazaki, Noda, Chiba, 278-8510, Japan
[c] School of Science and Engineering, Ehime University, 3, Bunkyo-cho, Matsuyama, Ehime 790-8577, Japan
Version of record first published: 02 Apr 2012.

To cite this article: Keiji Ogi , Shinji Ogihara & Yashiro Shigeki (2010): A Probabilistic SCG Model for Transverse Cracking in CFRP Cross-ply Laminates under Cyclic Loading, Advanced Composite Materials, 19:1, 1-17

To link to this article: http://dx.doi.org/10.1163/156855109X434784

VSP

Advanced Composite Materials 19 (2010) 1–17

ADVANCED COMPOSITE MATERIALS
brill.nl/acm

A Probabilistic SCG Model for Transverse Cracking in CFRP Cross-ply Laminates under Cyclic Loading

Keiji Ogi [a,*], **Shinji Ogihara** [b] **and Yashiro Shigeki** [a]

[a] School of Science and Engineering, Ehime University, 3, Bunkyo-cho, Matsuyama, Ehime 790-8577, Japan

[b] Faculty of Science and Technology, Tokyo University of Science, 2641, Yamazaki, Noda, Chiba, 278-8510, Japan

Received 3 July 2008; accepted 9 December 2008

Abstract

This paper presents a probabilistic fatigue model for transverse cracking in CFRP cross-ply laminates. First, a delayed fracture model for a crack in a brittle material subjected to cyclic loading was established on the basis of the slow crack growth (SCG) concept in conjunction with the Weibull's probabilistic failure model. Second, the above probabilistic delayed fracture model was applied to transverse cracking in cross-ply laminates during cyclic loading. The stress distribution and the length of the unit element were calculated with the aid of a shear lag analysis. The transverse crack density was expressed as a function of maximum stress, stress ratio and number of cycles using the parameters associated with the Paris equation and the Weibull distribution in addition to the mechanical properties. Unknown parameters were determined from experiment data for three kinds of cross-ply laminates to reproduce the transverse crack density against the number of cycles. The parametric studies using the obtained parameters revealed the effects of the Weibull modulus, crack propagation exponent and stress ratio on evolution of transverse cracking under fatigue loading.

Keywords

Composite laminate, transverse cracking, fatigue, probabilistic failure, delayed fracture

1. Introduction

As carbon fiber reinforced plastic (CFRP) laminates have been widely employed as lightweight structural materials of aircraft, automobile, wind power generators and in other applications, durability has been required increasingly in long-term practical use.

* To whom correspondence should be addressed. E-mail: kogi@eng.ehime-u.ac.jp
Edited by JSCM

DOI:10.1163/156855109X434784

Matrix cracking is usually the first microscopic damage observed in CFRP laminate during fatigue loading as well as during static loading. Transverse cracking behavior in cross-ply laminates has been investigated using the shear lag analysis and the energy principle based on fracture mechanics in the literature [1–5]. Time-dependent behavior in FRP laminates has also been studied, mostly on the basis of viscoelastic theories [6–10] where constitutive models were established to predict the creep deformation. Time-dependent transverse cracking behavior has been investigated experimentally by some researchers [11, 12] and analytically by the authors [13, 14] who have proposed a viscoelastic deformation model in conjunction with probabilistic transverse cracking.

Kaminski [15] has reviewed and classified fatigue models of composite materials into deterministic and stochastic ones. Many of the probabilistic models were based on Weibull statistics [16–21] and some of them were associated with the slow crack growth (SCG) concept [20, 21].

Nevertheless, little attention has been paid to a theoretical approach to fatigue transverse cracking in composite laminates. Ogin and co-workers [22, 23] employed a fracture mechanical approach to describe fatigue transverse crack evolution in GFRP cross-ply laminates using the Paris law. They assumed that the stress intensity factor for a transverse crack depends on the thickness and the average applied stress of the transverse ply when the crack is relatively long. In their model, a crack propagation rate as well as a stress intensity factor is independent of crack length. Lafarie-Frenot *et al.* identified the physical and geometrical parameters governing matrix cracking in CFRP laminates under cyclic loading [24]. Yokozeki *et al.* [25] also investigated fatigue matrix cracking behavior in cross-ply and quasi-isotropic laminates. They observed that transverse cracks propagate in the width direction simultaneously at its initiation on the edge surface in the cross-ply laminates. In the above literature [22–25], transverse cracks were observed to grow stably across the width on a millimeter scale during cyclic loading. However, when the transverse ply thickness is much larger than the initial and critical crack length, it is expected that an edge transverse crack propagates extensively in the width direction (or spans the width in a narrow specimen) at the same time as the initiation because the crack grows stably on the scale of 10 μm followed by unstable growth. The authors [26] have recently developed a probabilistic model to predict time-dependent transverse cracking in a cross-ply laminate under constant loading based on the SCG concept. In their model, a stress intensity factor of transverse crack depends on not only applied stress but also crack length since they assumed the micro-scale SCG. This model can be extended to the transverse cracking under arbitrary type of loading including cyclic loading.

This paper presents a fatigue model for transverse cracking in CFRP cross-ply laminates. First, a probabilistic fracture model for time-dependent crack propagation in a brittle material is briefly described. The failure probability is expressed as a function of the maximum stress $\sigma_{\max}$ and the number of cycles, N. The two-parameter Weibull distribution is employed here because the range of applied stress

is wider in the present study while the three-parameter Weibull distribution was employed for the applied stress around the lower limit of transverse strength in the previous work [26]. Next, the above model is applied to the fatigue behavior of transverse cracking in cross-ply laminates with various transverse ply thicknesses. The element size and the stress distribution are obtained with the aid of the shear lag analysis taking the residual stress into account. Finally, parametric studies were conducted to reveal the effect of the shape parameter, crack propagation exponent and stress ratio on the fatigue transverse cracking behavior.

2. Modeling

2.1. Probabilistic SCG Model

At first in this section, the SCG behavior of an initial crack under applied stress $\sigma(t)$ is formulated on the basis of the fracture mechanics model [27]. Then the probabilistic concept is incorporated with the SCG model [26]. The stress intensity factor K_{I} of a crack of length a is expressed as

$$K_{\mathrm{I}} = Y\sigma(t)\sqrt{a}, \tag{1}$$

where Y is a constant depending on the geometry of the crack. The Paris equation that describes the relationship between the crack propagation rate v and K_{I} is given by

$$v = \frac{\mathrm{d}a}{\mathrm{d}t} = A\left(\frac{K_{\mathrm{I}}}{K_{\mathrm{IC}}}\right)^n, \tag{2}$$

where A, n and K_{IC} denote a material constant, a crack propagation exponent and fracture toughness, respectively. We used K_{IC} instead of the stress intensity factor range ΔK_{I} because the effect of loading history is included in $\sigma(t)$. Now we consider a sinusoidal cyclic stress with the maximum stress of $\sigma_{\max}$, the period of τ and the stress ratio of R given by

$$\sigma(t) = \sigma_{\max}\left(\frac{1+R}{2} + \frac{1-R}{2}\sin\frac{2\pi t}{\tau}\right). \tag{3}$$

Summing up the integration of (2) using (1) N_{f} (the number of cycles to unstable crack growth) times, one obtains

$$a_0^{-(n-2)/2} - a_{\mathrm{f}}^{-(n-2)/2} = A\frac{n-2}{2}\left(\frac{Y}{K_{\mathrm{IC}}}\right)^n N_{\mathrm{f}}\int_0^{\tau}\{\sigma(t)\}^n\,\mathrm{d}t, \tag{4}$$

where a_0 and a_{f} denote the initial crack length and the crack length at N_{f} cycles, respectively. These crack lengths are related with the fracture toughness and the static strength S_i as

$$a_0 = \left(\frac{K_{\mathrm{IC}}}{YS_i}\right)^2 \tag{5}$$

and

$$a_{\mathrm{f}} = \left(\frac{K_{\mathrm{IC}}}{Y\sigma_{\max}}\right)^2. \tag{6}$$

Substitution of equations (3), (5) and (6) into equation (4) leads to

$$N_{\mathrm{f}} = \frac{1}{g(n, R)\tau\sigma_{\max}^2}\left\{\left(\frac{S_i}{\sigma_{\max}}\right)^{n-2} - 1\right\}, \tag{7}$$

with

$$g(n, R) = A\frac{n-2}{2}\left(\frac{Y}{K_{\mathrm{IC}}}\right)^2 \frac{1}{2\pi}\int_0^{2\pi}\left(\frac{1+R}{2} + \frac{1-R}{2}\sin\theta\right)^n \mathrm{d}\theta. \tag{8}$$

Thus, the parameter g contains the stress ratio R as well as the material constants A, n and K_{IC}.

Next we consider a brittle material with numerous cracks as initial defects. It is assumed that the brittle material (volume V) is decomposed into q elements (volume $V_{\mathrm{e}} = V/q$) and that each element has only one crack. When the static strength obeys the two-parameter Weibull distribution, the fracture probability of the material is expressed as

$$F(S_i) = 1 - \exp\left\{-V\left(\frac{S_i}{\alpha_{\mathrm{S}}}\right)^m\right\}, \tag{9}$$

where α_{S} and m denote scale and shape parameters.

Here it is assumed that all the initial cracks in the material independently grow without any interaction. The equivalent static strength S_i^* for the maximum stress of $\sigma_{\max}$ and the number of cycles N is obtained from (7) as

$$S_i^* = \left(1 + g(n, R)\sigma_{\max}^2\tau N\right)^{1/(n-2)}\sigma_{\max}. \tag{10}$$

Replacing S_i in (9) with S_i^* in (10) gives the fracture probability at $\sigma_{\max}$ and N as

$$F(\sigma_{\max}, N, V) = 1 - \exp\left[-V\left(1 + g(n, R)\sigma_{\max}^2\tau N\right)^{\kappa}\left(\frac{\sigma_{\max}}{\alpha_{\mathrm{S}}}\right)^m\right], \tag{11}$$

where $\kappa = m/(n-2)$ is a material constant including the SCG and probabilistic parameters.

When the applied stress $\sigma(t)$ is different from a cyclic one, the parameter g is also different from (8) because it includes the effect of loading history. However, the above formulation is applicable to arbitrary loading history through appropriate modification.

2.2. SCG Model of Transverse Cracking

Next, the delayed fracture model of transverse cracking in a cross-ply laminate under cyclic loading is established based on the same concept as in the previous work [26]. It is assumed that the laminate consists of unit elements (length L_{e}) that contain only one initial edge crack in the transverse ply as seen in Fig. 1(a). In the present model, L_{e} is assumed to be constant independent of the applied stress.

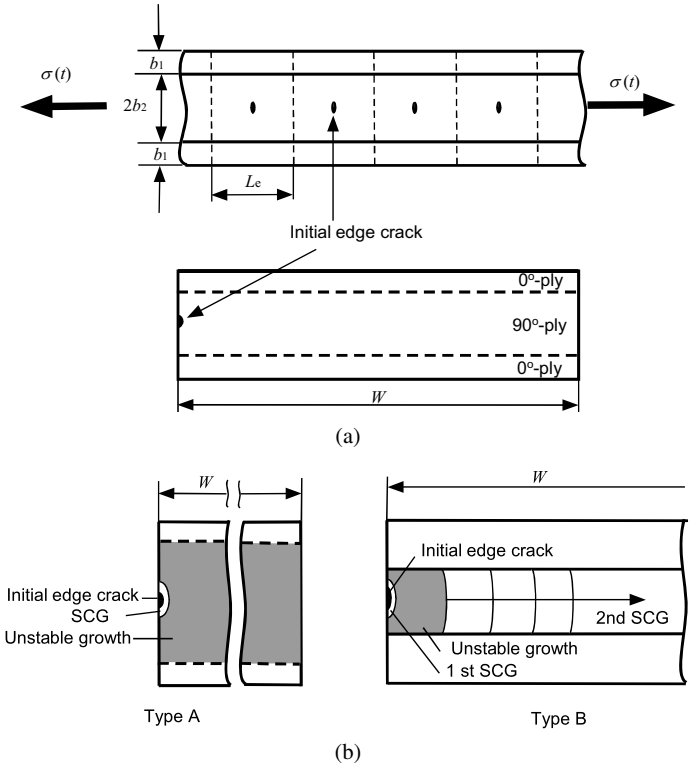

Figure 1. (a) Unit elements and (b) two types of crack growth in the SCG model for transverse cracking in a cross-ply laminate.

Figure 1(b) shows a schematic of two types (stable and unstable) of transverse crack growth in a cross-ply laminate. The initial crack grows stably on the scale of 10 μm followed by unstable growth across the width in Type A while it propagates stably across the width on the millimeter scale after initiation of a through-the-thickness edge transverse crack in Type B. It depends on the transverse ply thickness $2b_2$ and width of the specimen W which type is dominant. When the transverse ply is thin, the crack grows stably in the mode of Type B undergoing constraint from the longitudinal plies. In contrast, when the transverse ply is relatively thick, the crack tends to propagate unstably across the width in the mode of Type A and sometimes spans the width for a narrow specimen. In the present study, transverse crack propagation of Type A is assumed supposing that the transverse ply is thick and the specimen is narrow. The reasonableness of this assumption was confirmed by the fact that the estimated initial and critical crack lengths were smaller than the thickness of one ply (about 120 μm) [26].

The number of cycles to unstable growth of initial crack in each unit element depends on the initial crack length. The length of the unit element should be long enough for the initial cracks to propagate independently. This length is de-

termined on the basis of the shear lag model [26]. The maximum applied stress in the transverse ply is assumed to be constant although the actual stress decreases with increasing transverse crack density [26].

The probabilistic expression of transverse crack density is given by

$$\rho = \rho_S F(\sigma_{2,\max}, N, V_e), \tag{12}$$

where $\rho_S = L_e^{-1}$, $F(\sigma_{2,\max}, N, V_e)$ and $\sigma_{2,\max}$ represent the saturated transverse crack density, the fracture probability and the maximum stress in the transverse ply, respectively. The equivalent static stress in the transverse ply S_i^* is expressed from (10) as

$$S_i^* = \left(1 + g(n, R)\sigma_{2,\max}^2 \tau N\right)^{1/(n-2)} \sigma_{2,\max}. \tag{13}$$

The stress $\sigma_{2,\max}$ is decomposed into the maximum applied stress $\sigma_{\max}$ in the laminate and the thermal residual stress σ_2^T in the transverse ply as

$$\sigma_{2,\max} = r\sigma_{\max} + \sigma_2^T, \tag{14}$$

with

$$r = \frac{(b_1 + b_2)E_2}{b_1 E_1 + b_2 E_2}, \tag{15}$$

where b_i is the half thickness and E_i the Young's modulus of the longitudinal ($i = 1$) and transverse ($i = 2$) plies. Combining equations (11) and (12), we obtain

$$\frac{\rho}{\rho_S} = 1 - \exp\left[-V_e\left(1 + g(n, R)\sigma_{2,\max}^2 \tau N\right)^{\kappa} \left(\frac{\sigma_{2,\max}}{\alpha_S}\right)^m\right]. \tag{16}$$

Thus, the transverse crack density ρ can be predicted from (16) using the material constants and the loading parameters (R, $\sigma_{2,\max}$ and τ).

One of the advantages of this model is to be able to predict the transverse crack density probabilistically by means of the Paris law describing SCG behavior. Equation (16) expresses the transverse crack density explicitly as a function of the number of cycles N and the maximum stress $\sigma_{2,\max}$ through the use of the Weibull and SCG parameters (m and n). Another advantage is that the equation includes the effect of stress ratio R and period τ of cyclic loading in addition to the effect of stacking sequence, which is involved in V_e and ρ_S.

2.3. Determination of Material Constants

The shape and scale parameters m and α_S in the two-parameter Weibull distribution were determined from the tensile test of 90° specimens [4]. Here, α_S was recalculated to give the best fitting to ρ–N data at the early stage of the fatigue test of cross-ply laminates [5].

Next, n and g were determined using the ρ–N data of cross-ply laminates in the fatigue test [5] as follows. Equation (16) is rewritten as

$$\ln\left\{\ln\left(\frac{\rho_S}{\rho_S-\rho}\right)\right\} - m\ln\frac{\sigma_{2,\max}}{\alpha_S} - \ln V_e = \kappa\ln(1+g\sigma_{2,\max}^2\tau N). \qquad (17)$$

First, the experimental data on the left side of (17) were plotted against $x = \sigma_{2,\max}^2\tau N$ for all kinds of cross-ply laminates. Then n and g were provided through the curve fitting of these plots to the equation $y = \kappa\ln(1+gx)$.

The saturated transverse crack density ρ_S is defined as the inverse of the element length, which was estimated from the static tensile test as $\rho_S = 1.24$, 0.928 and 0.795/mm for $p = 4, 8$ and 12, respectively. This means that the transverse ply stress σ_2 at the middle of the element equals 92% of the original value from zero at the crack surface, σ_{20} (see Appendix 1).

3. Verification of the Model

3.1. Experimental Data

In this section, the model is verified using the experimental data and the material constants given in the literature [4, 5]. The material used in the experiment was carbon/epoxy (T800H/#3631, Toray) cross-ply laminates with three different stacking sequences $[0°/90°_p/0°]$ ($p = 4, 8, 12$). The specimens with the gage length L_G of 30 mm and the width W of 3.0 mm were used for both static tensile and fatigue tests. The fatigue tests were performed at the stress ratio R of 0, the frequency of 5 Hz ($\tau = 0.2$ s) and the ratio of maximum applied stress $\sigma_{\max}$ to static strength σ_B, denoted by s, of 0.40, 0.50, 0.60, 0.80 and 0.95. However, the data for $s = 0.40$ were excluded in the data fitting because the transverse crack density was much lower than one for higher s. In addition, the data measured only at room temperature were employed throughout, even though experiments were conducted also at an elevated temperature. This is because the effect of delamination becomes more dominant at the elevated temperature. For the same reason, the data for $s = 0.95$ of the laminate with $p = 12$ was also excluded in the fitting procedure. The material properties and the dimensions of the specimens for each laminate are listed in Table 1. Thermal residual stress σ_2^T estimated by means of a ply separation method [4] was adopted for accurate evaluation.

3.2. Results and Verification of the Model

Figure 2 presents experiment results as ρ–N diagrams for each cross-ply laminate under fatigue loading [5]. When the maximum stress to strength ratio s is high, transverse crack density ρ starts to increase from the lower number of cycles and increases up to relatively high values. Small transverse crack density for $s = 0.95$ of $p = 12$ is ascribed to delamination growth as will be discussed later. In the case

Table 1.
Material properties, geometric parameters of specimens and maximum applied stress in the transverse plies [4, 5]

p	4	8	12	
E_1 (GPa)	152.2			
E_2 (GPa)	9.57			
$2b_1$ (mm)	0.27			
$2b_2$ (mm)	0.54	1.08	1.62	
L_G (mm)	30			
W (mm)	3			
G/d_0 (GPa/mm)	90.7			
m	7.69			
n	21.7*			
$g(n, 0)$ (MPa^{-2} s^{-1})	4.94×10^{-4}*			
A (m/s)	2.60×10^{-4}*#			
K_{IC} (MPa$\sqrt{\text{m}}$)	1.4**			
α_S (MPa)	197*			
r	0.168	0.251	0.320	
ξ (mm^{-1})	6.28	4.69	4.01	
ρ_S (mm^{-1})	1.24*	0.928*	0.795*	
V_e (mm^3)	1.30*	3.49*	6.12*	
σ_B (MPa)	770	480	325	
σ_2^T (MPa)	24.1	21.6	19.7	
$\sigma_{2,\max}$ (MPa)	$s = 0.5$	88.8	81.8	71.9
	$s = 0.6$	101.7	93.9	81.1
	$s = 0.8$	127.6	118.0	102.9
	$s = 0.95$	147.1	136.1	118.6

Values, except for the following, are given in Refs [4, 5]: *values obtained in the present study and #value assuming $Y = \sqrt{\pi}$, **value in Ref. [28].

of low s, transverse cracking does not take place until high N and the increment in ρ is small. As the transverse ply is thicker (p is larger), ρ begins to increase at higher N and its increment is smaller.

Figure 3 plots the experimental data of x and y together with the fitted curve based on (17). This curve fitting offers $g = 4.94 \times 10^{-4}$ (MPa^{-2} s^{-1}) and $n = 21.7$. The estimated crack propagation exponent n is in reasonably good agreement with the reference data $n = 18, 29$ ($R = 0.2, 0.5$) for fatigue mode-I delamination propagation of the same material [28].

The transverse crack density *versus* the number of cycles reproduced by means of all the material constants in Table 1 inserted into equation (16) is denoted by the solid and dotted lines in Fig. 2. The reproductions are in reasonably good agreement with the experiment results. However, the model overestimates the transverse crack density for smaller s and larger p (thicker transverse ply). This discrepancy is discussed in the next section.

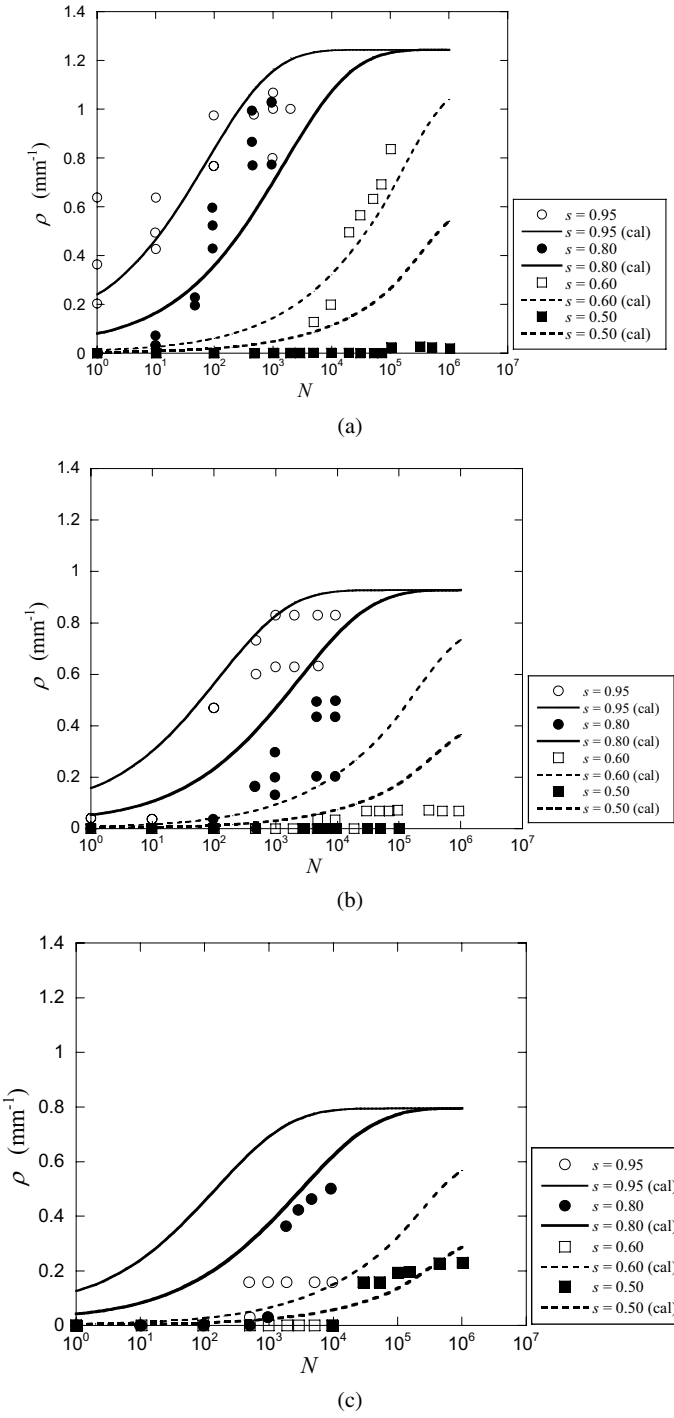

Figure 2. Measured and predicted transverse crack density in three kinds of cross-ply laminates under fatigue loading with various stress ratios. (a) $p = 4$, (b) $p = 8$ and (c) $p = 12$.

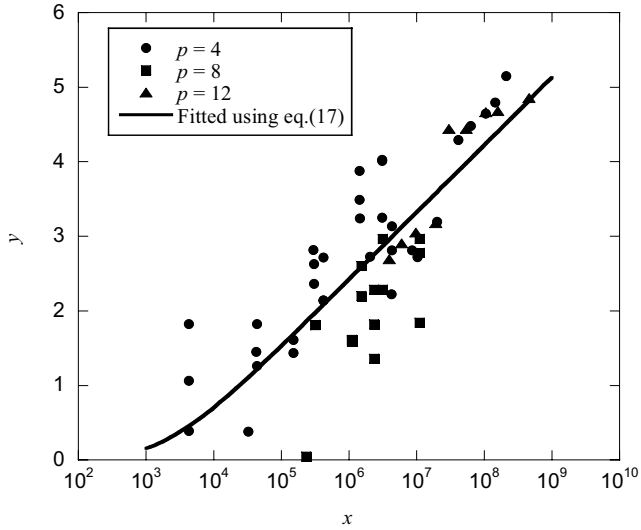

Figure 3. Measured and fitted values of *y versus x* in (17).

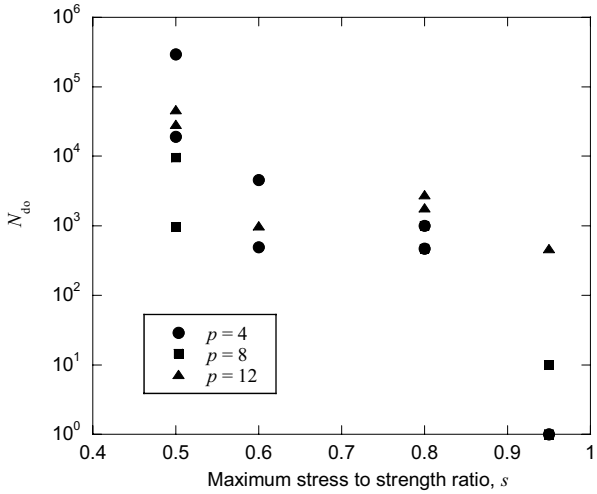

Figure 4. Number of cycles at the delamination onset *versus* the applied stress to strength ratio in three kinds of laminates.

4. Discussion

4.1. Problems

First, the interaction between delamination and transverse cracking is discussed in seeking an explanation of the above discrepancy. Figure 4 shows the number of cycles at delamination onset N_{do} *versus* the maximum applied stress to strength ratio s in the cross-ply laminates with different transverse ply thickness [5]. Delamination takes place earlier with increasing s although a large difference among

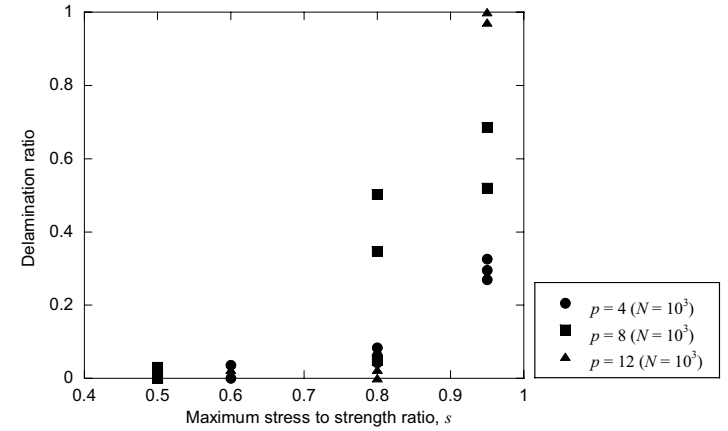

(a)

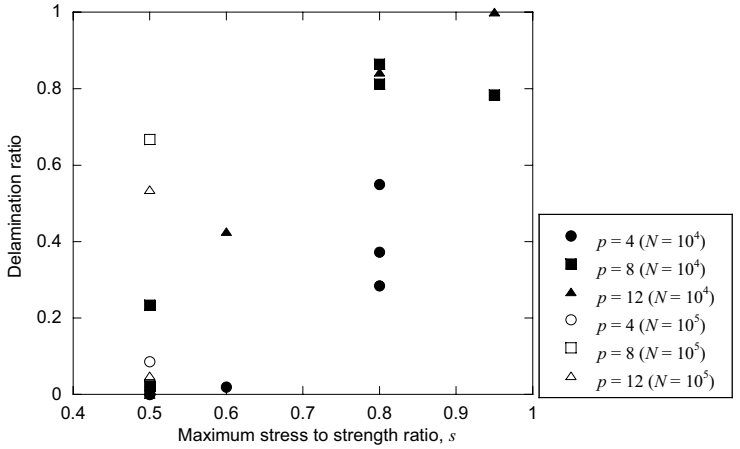

(b)

Figure 5. Delamination ratio *versus* the applied stress to strength ratio in three kinds of laminates at (a) $N = 10^3$ and (b) $N = 10^4$ and 10^5.

the laminates is not observed. Figure 5 shows the delamination ratio, defined as the ratio of total delamination length to the total interlaminar length (the element length), against s in three kinds of laminates at (a) $N = 10^3$ and (b) $N = 10^4$ and 10^5. It is found that delamination grows longer as the applied stress is higher or the transverse ply is thicker. Comparing the delamination onset and growth behavior in Figs 4 and 5 with the transverse cracking behavior in Fig. 2, it is proved that the evolution of delamination and the transverse cracking overlapped each other during cyclic loading. Hence, delamination affects transverse cracking especially in the case of high applied stress or thick transverse ply where delamination is relatively long. Generally, delamination suppresses transverse cracking because it interrupts the stress transfer to the transverse ply. From the above discussion, it is concluded that the transverse crack density lower than predicted one for $p = 8, 12$ is mainly

due to the delamination growth. The model considering the delamination should be established for more accurate prediction.

The disagreement in the case of small s is caused by the Weibull distribution without the lower limit of the transverse strength σ_{2L} that was introduced as one of the three Weibull parameters in Ref. [26]. The value of σ_{2L} is estimated to be 80–100 MPa depending on the transverse ply thickness [4]. These values are comparable to the maximum transverse ply stress $\sigma_{2,\max}$ for $s = 0.5$ and $s = 0.6$ of each laminate. In this stress range, the effect of σ_{2L} on SCG becomes remarkable. Indeed, the three-parameter Weibull distribution can explain more clearly the delayed fracture phenomena that transverse cracking takes place only after some cycles. However, we employed the two-parameter Weibull distribution to cope with the wider stress range in the present study. Consequently, agreement is poor in the case of $s = 0.5$ and $s = 0.6$.

Another reason for the discrepancy in the case of small s is thought to be the existence of the upper limit of the fracture probability $F_{\max}$. When the maximum stress is relatively small, some initial cracks do not propagate during cyclic loading because their stress intensity factor is kept to be smaller than threshold one K_{th} (see Appendix 2). The upper limit of transverse crack density ρ_{th} and the number of cycles to ρ_{th}, denoted by N_{th}, are obtained from equations (A4) and (16) as

$$\rho_{th} = \left[1 - \exp\left\{-V_e\left(\frac{\sigma_{2,\max}}{\alpha_S}\frac{K_{IC}}{K_{th}}\right)^m\right\}\right]\rho_S \tag{18}$$

and

$$N_{th} = \frac{(K_{IC}/K_{th})^{n-2} - 1}{g\tau\sigma_{2,\max}^2}, \tag{19}$$

respectively. Assuming that K_{IC}/K_{th} is equal to the one for mode I delamination ($K_{IC}/K_{th} = 1.64$) [28], N_{th} is estimated to be 7.9×10^3–2.2×10^4 for $p = 4$ ($s =$ 0.95–0.5) and 1.1×10^4–2.9×10^4 for $p = 8$ ($s = 0.95$–0.5). For high stress ratio s, transverse crack density ρ increases thoroughly by N_{th} and the influence of K_{th} is limited. However, ρ does not increase any more after reaching ρ_{th} at N_{th} for low s. If $K_{IC}/K_{th} = 2$ is employed, the effect of K_{th} is negligible since N_{th} is 3.9×10^4 even for the largest $\sigma_{2,\max}$ ($p = 4$, $s = 0.95$).

4.2. Parametric Study

In this section the effect of the shape parameter or Weibull modulus m, crack propagation exponent n, and stress ratio R on the transverse cracking behavior was investigated. A simulation was carried out for the laminate of $p = 4$ in the case of $s = 0.95$ and 0.60. Numerical integration was conducted in calculation of $g(n, R)$ (equation (8)).

The calculated ρ–N curves are depicted in Fig. 6 where the Weibull modulus m was varied from 5 to 20 keeping n and R constant ($n = 20$, $R = 0$). In this case, g remains constant according to (8). As the value of m becomes larger, the initial

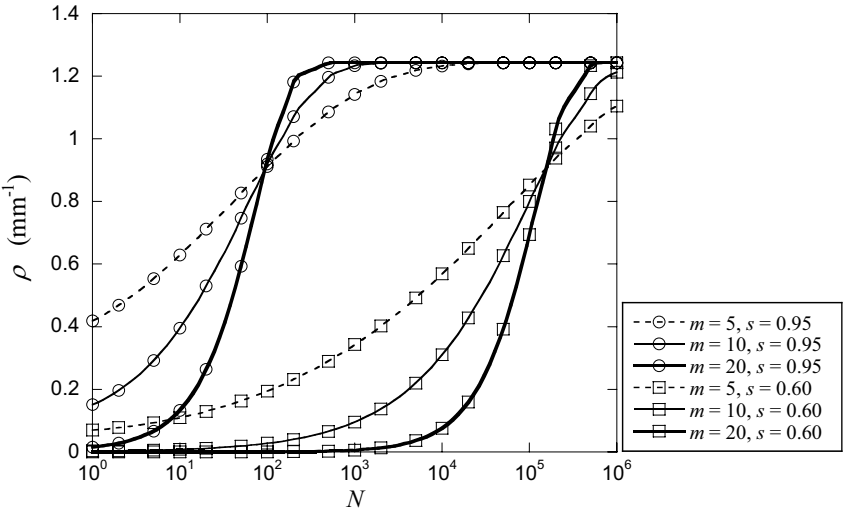

Figure 6. Effect of the Weibull modulus on transverse crack density ρ-number of cycles N curves in cross-ply laminates under fatigue loading ($n = 20$, $R = 0$).

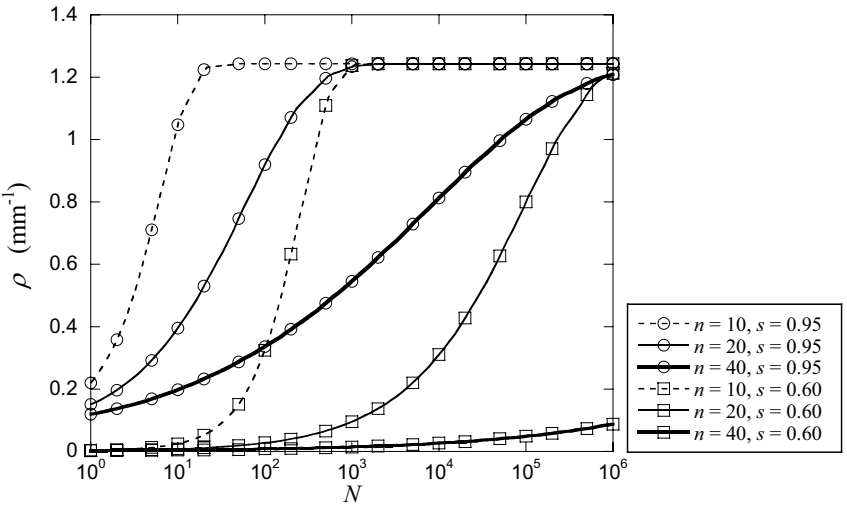

Figure 7. Effect of the crack propagation exponent on transverse crack density ρ-number of cycles N curves in cross-ply laminates under fatigue loading ($m = 10$, $R = 0$).

transverse crack density at $N = 1$ becomes smaller, but it increases more rapidly up to the saturated one ρ_S. This is because the larger Weibull modulus means the narrower variation of the initial crack length and the equivalent transverse strength (equation (10)).

Figure 7 shows the effect of crack propagation exponent n on ρ–N curves ($m = 10$, $R = 0$). The value of g increases monotonically with an increase in n. The initial ρ becomes larger and the number of cycles to ρ_S becomes smaller as n becomes

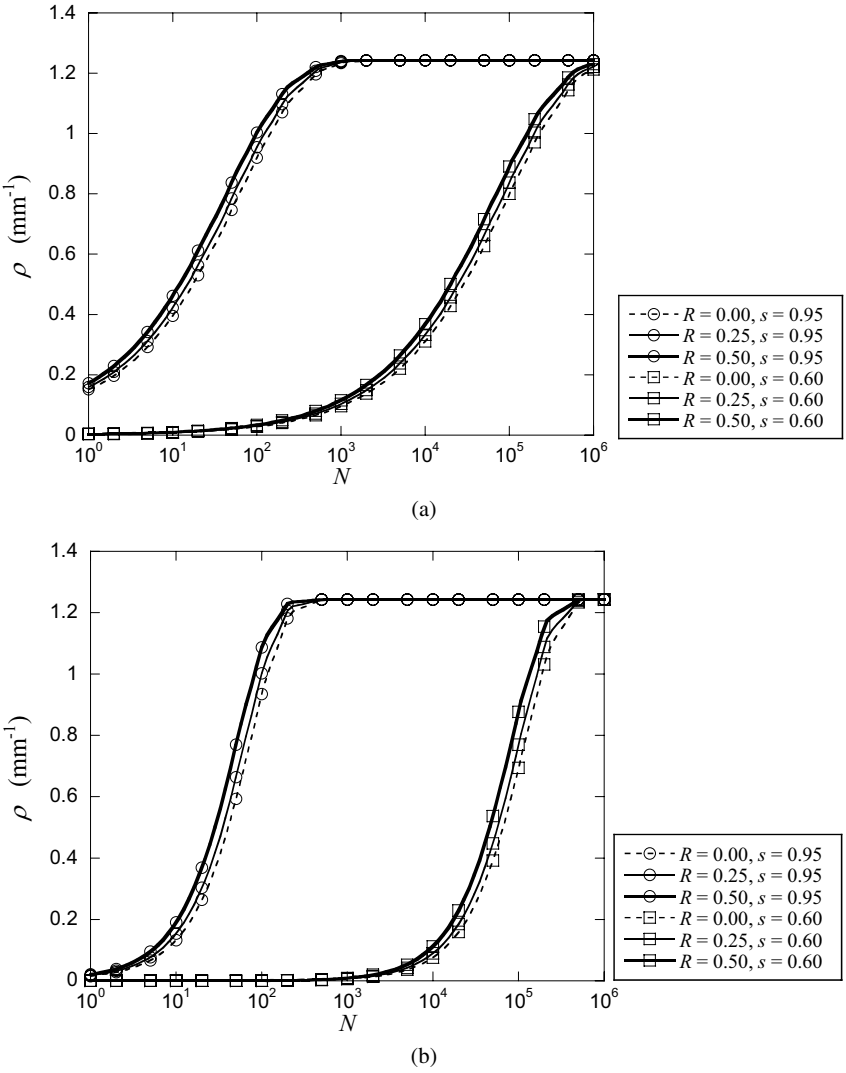

Figure 8. Effect of the stress ratio on transverse crack density ρ-number of cycles N curves in cross-ply laminates under fatigue loading. (a) $\kappa = 0.556$ ($m = 10$, $n = 20$), (b) $\kappa = 1.111$ ($m = 20$, $n = 20$).

smaller in the curves for $s = 0.95$. Similar behavior is observed for $s = 0.60$ though the increase in ρ is very limited in the case of $n = 40$. This result is reasonable because crack propagation becomes slower as n becomes larger.

Figure 8 shows the transverse crack density for various stress ratio R for (a) $(m, n) = (10, 20)$ ($\kappa = 0.556$) and (b) $(m, n) = (20, 20)$ ($\kappa = 1.111$). The transverse crack density ρ as well as g increases with increasing R while the number of cycles to ρ_S is hardly affected by R. The effect of R on ρ is more prominent and the rate of increase in ρ is larger in Fig. 8(b) than in Fig. 8(a). The value of g

for $R = 0.5$ is 1.4 times as large as g for $R = 0$. The degree of influence of R is affected by the exponent of $1 + g\sigma_{2,\max}^2 \tau N$, κ (see equation (16)). Accordingly, the large difference between $R = 0.5$ and 0 is observed in (b) where κ is larger than unity, while the effect of R is limited in (a) with smaller κ.

5. Conclusions

A probabilistic model for predicting transverse crack density in CFRP cross-ply laminates under cyclic loading was established based on the fracture mechanics and the SCG concept. The transverse crack density was given as a function of maximum stress, stress ratio and number of cycles using the parameters associated with the Weibull distribution and the Paris equation. The predictions were compared with the experimental results for three kinds of cross-ply laminates with different transverse ply thickness. The validity of the model was confirmed although some discrepancy was observed in the case of low maximum applied stress ratio and thick transverse ply. Parametric studies revealed the effect of the shape parameter, crack propagation exponent and stress ratio on the delayed transverse cracking behavior.

References

1. J. E. Masters and K. L. Reifsneider, An investigation of cumulative damage development in quasi-isotropic graphite/epoxy laminates, in: *Damage in Composite Laminates*, ASTM STP 775, pp. 40–62. American Society for Testing and Materials, Philadelphia, USA (1982).
2. A. S. D. Wang, Fracture mechanics of sublaminate cracks in composite materials, *Compos. Technol. Rev.* **6**, 45–62 (1984).
3. J. A. Nairn, *Microcracking, microcrack-induced delamination, and longitudinal splitting of advanced composite structures*, NASA CR4472. National Aeronautics and Space Administration, Washington, DC, USA (1992).
4. N. Takeda and S. Ogihara, *In situ* observation and probabilistic prediction of microscopic failure processes in CFRP cross-ply laminates, *Compos. Sci. Technol.* **52**, 183–195 (1994).
5. N. Takeda, S. Ogihara and A. Kobayashi, Microscopic fatigue damage progress in CFRP cross-ply laminates, *Composites* **26**, 859–867 (1995).
6. Y. C. Lou and R. A. Shapery, Viscoelastic characterization of a nonlinear fiber-reinforced plastic, *J. Compos. Mater.* **5**, 208–234 (1971).
7. D. L. Flaggs and F. W. Crossman, Analysis of the viscoelastic response of composite laminates during hygrothermal exposure, *J. Compos. Mater.* **45**, 21–40 (1981).
8. D. A. Dillard, D. H. Morris and H. F. Brinsson, Predicting viscoelastic response and delayed failures in general laminated composites, in: *Composite Materials: Testing and Design (Sixth Conference)*, ASTM STP 787, I. M. Daniel (Ed.), pp. 357–370. American Society of Testing and Materials, Philadelphia, USA (1982).
9. A. Horoschenkoff, Characterization of creep compliances J22 and J66 of orthotropic composites with PEEK and epoxy matrices using the nonlinear viscoelastic response of the neat resins, *J. Compos. Mater.* **24**, 879–891 (1990).
10. I. Chung, C. T. Sun and I. Y. Chang, Modeling creep in thermoplastic composites, *J. Compos. Mater.* **27**, 1009–1029 (1993).

11. R. H. Moore and D. A. Dillard, Time-dependent matrix cracking in cross-ply laminates, *Compos. Sci. Technol.* **39**, 1–12 (1990).
12. J. Raghavan and M. Meshii, Time-dependent damage in carbon fibre-reinforced polymer composites, *Composites A* **27A**, 1223–1227 (1996).
13. K. Ogi and Y. Takao, Evolution of transverse cracking in CF/epoxy cross-ply laminates under creep loading, *J. Reinf. Plast. Compos.* **18**, 1220–1230 (1999).
14. K. Ogi and Y. Takao, Modeling of time-dependent behavior of deformation and transverse cracking in cross-ply laminates, *Adv. Compos. Mater.* **10**, 39–62 (2001).
15. M. Kaminski, On probabilistic fatigue models for composite materials, *Intl J. Fatigue* **24**, 477–495 (2002).
16. G. Caprino and A. D'Amore, Flexural fatigue behaviour of random continuous-fibre-reinforced thermoplastic composites, *Compos. Sci. Technol.* **58**, 957–965 (1998).
17. H. Shen, J. Lin and E. Mu, Probabilistic model on stochastic fatigue damage, *Intl J. Fatigue* **22**, 569–572 (2000).
18. N. H. Tai, C. C. M. Ma and S. H. Wu, Fatigue behavior of carbon fibre/PEEK composites, *Composites* **26**, 551–559 (1995).
19. N. Chawla, M. Kerr and K. K. Chawla, Monotonic and cyclic fatigue behavior of high-performance ceramic fibers, *J. Amer. Ceram. Soc.* **88**, 101–108 (2005).
20. N. Iyengar and W. A. Curtin, Time-dependent failure in fiber-reinforced composites by fiber degradation, *Acta Materilia* **45**, 1489–1502 (1997).
21. R. Christensen and Y. Miyano, Stress intensity controlled kinetic crack growth and stress history dependent life prediction with statistical variability, *Intl J. Fracture* **137**, 77–87 (2006).
22. S. L. Ogin, P. A. Smith and P. W. R. Beaumont, A stress intensity factor approach to the fatigue growth of transverse ply cracks, *Compos. Sci. Technol.* **24**, 47–59 (1985).
23. L. Boniface and S. L. Ogin, Application of the Paris equation to the fatigue growth of transverse ply cracks, *J. Compos. Mater*. **23**, 735–754 (1989).
24. M. C. Lafarie-Frenot, C. Henaff-Gardin and D. Gamby, Matrix cracking induced by cyclic ply stresses in composite laminates, *Compos. Sci. Technol.* **61**, 2327–2336 (2001).
25. T. Yokozeki, T. Aoki and T. Ishikawa, Fatigue growth of matrix cracks in the transverse direction of CFRP laminates, *Compos. Sci. Technol.* **62**, 1223–1229 (2002).
26. K. Ogi, S. Yashiro, M. Takahashi and S. Ogihara, A probabilistic static fatigue model for transverse cracking in CFRP cross-ply laminates, *Compos. Sci. Technol.* **69**, 469–476 (2009).
27. A. G. Evans and E. R. Fuller, Crack propagation in ceramic materials under cyclic loading conditions, *Metall. Trans.* **5**, 27–33 (1974).
28. M. Hojo, S. Ochiai, C.-G. Gustafson and K. Tanaka, Effect of matrix resin on delamination fatigue crack growth in CFRP laminates, *Engng Fract. Mech.* **49**, 35–47 (1994).

Appendix 1: Shear Lag Analysis

When one transverse crack exists in an infinitely long coupon, the stress at a distance x from the transverse crack in the transverse ply is

$$\sigma_2(x) = \sigma_{20}\{1 - \exp(-\xi x)\}, \tag{A1}$$

where $\sigma_{20} = r\sigma_0 + \sigma_2^{\mathrm{T}}$ and ξ is a shear lag parameter expressed as

$$\xi = \sqrt{\frac{G(b_1E_1 + b_2E_2)}{b_1b_2d_0E_1E_2}}, \tag{A2}$$

where G and d_0 denote the shear modulus and the thickness of the interlaminar shear layer, respectively [4]. Here, the element length L_e is defined as the double of x. By substituting $x = L_e/2 = 1/(2\rho_S)$ in equation (A1) together with $\rho_S = 1.24$, 0.928 and 0.795/mm, we obtain $\sigma_2/\sigma_{20} = 0.92$.

Appendix 2: Threshold Stress Intensity Factor

When the stress intensity factor of an initial crack (length a_{th}) instantaneously becomes the threshold one K_{th} for a given maximum stress σ_{max}, K_{th} is expressed as

$$K_{th} = Y\sigma_{max}\sqrt{a_{th}}. \tag{A3}$$

Only the initial cracks longer than a_{th} show SCG behavior. Then the upper limit of fracture probability F_{max} is given by

$$F_{max} = 1 - \exp\left\{-V\left(\frac{\sigma_{max}}{\alpha_S}\frac{K_{IC}}{K_{th}}\right)^m\right\}. \tag{A4}$$

Substitution of $F = F_{max}$ in (11) gives the threshold number of cycles as equation (19).